Destabilization of Magnetic Order in a Dilute Kitaev Spin Liquid Candidate

P. Lampen-Kelley, A. Banerjee, A. A. Aczel, H. B. Cao, M. B. Stone, C. A. Bridges, J.-Q. Yan, S. E. Nagler, and D. Mandrus

Phys. Rev. Lett. **119**, 237203 — Published 6 December 2017

DOI: 10.1103/PhysRevLett.119.237203

Destabilization of magnetic order in a dilute Kitaev spin liquid candidate

P. Lampen-Kelley,[1,2] A. Banerjee,[3] A.A. Aczel,[3] H.B. Cao,[3] M.B. Stone,[3] C.A. Bridges,[4] J.-Q. Yan,[2] S.E. Nagler,[3] and D. Mandrus[1,2]

[1]*Department of Materials Science and Engineering, University of Tennessee, Knoxville, TN 37996, U.S.A.*
[2]*Materials Science and Technology Division, Oak Ridge National Laboratory, Oak Ridge, TN, 37831, U.S.A.*
[3]*Neutron Scattering Division, Oak Ridge National Laboratory, Oak Ridge, TN 37831, U.S.A.*
[4]*Chemical Sciences Division, Oak Ridge National Laboratory, Oak Ridge, TN 37831, U.S.A.*

(Dated: November 8, 2017)

The insulating honeycomb magnet α-$RuCl_3$ exhibits fractionalized excitations that signal its proximity to a Kitaev quantum spin liquid (QSL) state, however, at $T = 0$, fragile long-range magnetic order arises from non-Kitaev terms in the Hamiltonian. Spin vacancies in the form of Ir^{3+} substituted for Ru are found to destabilize this long-range order. Neutron diffraction and bulk characterization of $Ru_{1-x}Ir_xCl_3$ show that the magnetic ordering temperature is suppressed with increasing x and evidence of zizag magnetic order is absent for $x > 0.3$. Inelastic neutron scattering demonstrates that the signature of fractionalized excitations is maintained over the full range of x investigated. The depleted lattice without magnetic order thus hosts a spin-liquid-like ground state that may indicate the relevance of Kitaev physics in the magnetically dilute limit of $RuCl_3$.

PACS numbers: 75.30.Kz, 75.10.Kt

The quantum spin liquid (QSL) holds particular fascination as a state of matter that exhibits strong quantum entanglement yet is devoid of long-range order [1, 2]. These exotic states can possess topologically protected fractionalized excitations, with possible implications for quantum information science [3, 4]. A prototypical example is the Kitaev model on a honeycomb lattice [5], which can be solved exactly and has a QSL ground state. An effective Hamiltonian with Kitaev terms consisting of bond-directional Ising couplings may arise in spin-orbit assisted Mott insulators with $J_{eff} = 1/2$ moments in an edge-sharing octahedral environment [6]. A strong push for the experimental realization of quasi-2D honeycomb lattices showing Kitaev physics initially focused on iridate materials with the chemical formula A_2IrO_3 [7–10], and more recently α-$RuCl_3$ [11–16]. Each of these compounds orders magnetically at low temperatures in a zigzag or incommensurate phase [17–23], and the effective low energy Hamiltonian is believed to be described by a generalized Heisenberg-Kitaev-Γ model [24–35]. Despite the appearance of long-range order, broad scattering continua observed via inelastic neutron or Raman scattering in α-$RuCl_3$ [13, 36–38] and the iridates [39] match the predicted signatures of itinerant Majorana fermions in pure Kitaev calculations [40–42], suggesting that these materials are proximate to the QSL state and that Kitaev interactions play an important role.

In this letter, we report the evolution of the magnetic ground state in α-$RuCl_3$ with magnetic Ru^{3+} substituted by nonmagnetic Ir^{3+}, and determine a phase diagram as a function of temperature and dilution. The motivation is two-fold: to understand the role of defects in Kitaev-candidate materials and to explore avenues towards suppression of long-range order. Numerous theoretical studies predict the emergence of novel superconductivity with hole doping in the strong Kitaev limit [43–49] while bond disorder [50], dislocations [51], magnetic impurities [52], and spin vacancies [53–60] have also received theoretical attention. Experimentally, substitution of both magnetic and non-magnetic cations for Ir rapidly led to spin glass freezing in Na_2IrO_3 and Li_2IrO_3 [61, 62]. Isoelectronic substitution within the solid solution $(Na,Li)_2IrO_3$ decreased the magnetic ordering temperature, although phase separation has hampered efforts to completely suppress long-range order [63–65].

The chemically simpler binary compound α-$RuCl_3$ provides an excellent framework to explore the effects of various perturbations on the relevant physics. Low-spin $5d^6$ $Ir^{3+}(S = 0)$ represents a non-magnetic impurity in the $J_{\text{eff}} = 1/2$ Ru^{3+} magnetic sublattice while the identical ionic radii (0.68 Å) of Ru^{3+} and Ir^{3+} preserve a regular MCl_6 environment (M = Ru, Ir) [66].

The van der Waals bonded honeycomb layers in α-$RuCl_3$ are susceptible to stacking faults that are known to affect the magnetic ordering properties. Single crystals without stacking faults show zigzag order with $T_N \simeq 7$ K and a three-fold (ABC) out- of-plane periodicity. With stacking faults, a phase with two-fold periodicity (ABAB) also appears at $T_N \simeq 14$ K [13–16, 22, 23]. Polycrystalline material shows only the 14 K transition. Our present study of $Ru_{1-x}Ir_xCl_3$ reveals the suppression of the ABC and ABAB magnetic phases with critical concentrations of $x \simeq 0.1$ and $x \simeq 0.3$, respectively, demonstrating that site dilution represents a viable approach to destabilizing long-range magnetic order. Spectroscopic examination of the magnetically disordered limit reveals a dynamic ground state with indications of persistent fractionalization of spin excitations.

Figure 1(a) shows the magnetic susceptibility of a series of $Ru_{1-x}Ir_xCl_3$ single crystals with magnetic field applied in the honeycomb *ab* plane. In addition to the $T_{N1} = 7$ K zigzag transition of the parent compound, a

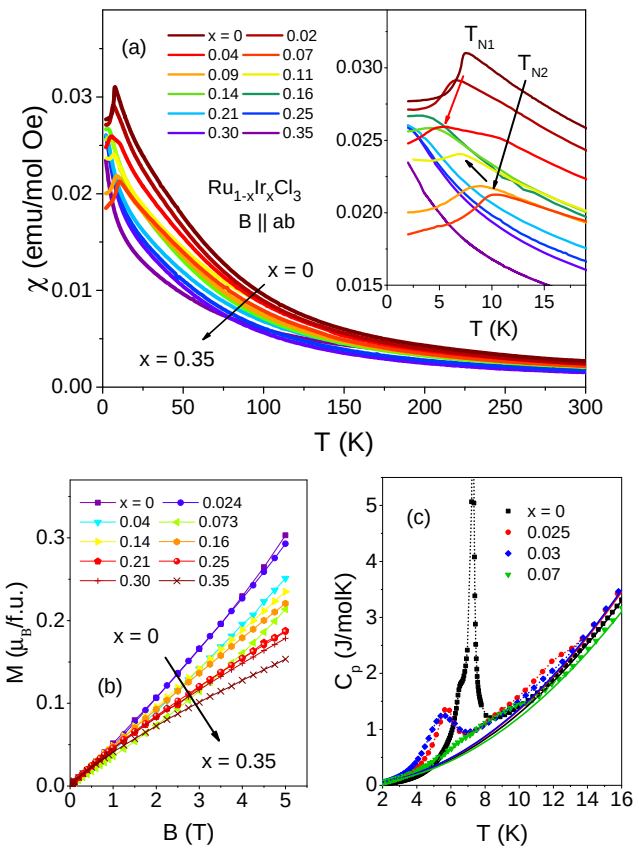

FIG. 1. (a) Magnetic susceptibility curves of $Ru_{1-x}Ir_xCl_3$ single crystals (x values indicated in legend) with a magnetic field of $B = 1$ T applied in the ab plane. Inset: magnification of low-temperature range. Red arrow and black/grey arrows mark the evolution of T_{N1} and T_{N2}, respectively. (b) Field-dependent magnetization at 2 K. The data of (a) and (b) with normalization to Ru content are shown in Supplementary Fig. S7. (c) Heat capacity curves of crystals with small Ir concentration. Solid lines are an estimate of the lattice contribution. Dotted lines are a guide to the eye.

second feature at $T_{N2} \leq 14$ K for $x > 0$ (black arrow, Fig.1a Inset) indicates that substituted crystals obtained from the current growth process are not completely free of stacking faults. The sharp cusp in the susceptibility at T_{N1} is rapidly shifted toward lower temperatures at non-zero x (red arrow) denoting a suppression of the ordering temperatures with dilution. As x increases, the minority phase contribution (T_{N2}) gains prominence and is the only transition evident above 2 K by $x = 0.09$. Further Ir substitution leads to a rounding of the cusp at T_{N2}, which decreases continuously with x and disappears near the percolation limit of the honeycomb lattice, $x \sim 0.3$ [67]. Notably, field-cooled and zero-field-cooled measurements are identical for all values of x, in contrast to the spin-glass-like characteristics reported in the honeycomb iridates with non-magnetic substitution [64]. In fact, muon spin relaxation (μSR) experiments rule out a glassy state and point to fast dynamics on the μSR time scale ($10^4 - 10^{12}$ Hz) in the magnetically disordered limit [see Supplementary Information (SI) Fig. S4 and S9, and discussion including Refs. [68, 69]].

The low-temperature susceptibility does not decrease monotonically with x, but instead increases over the range $0.07 < x < 0.16$. This behavior might arise from uncompensated moments introduced by nonmagnetic impurities in the ordered antiferromagnetic ground state of the parent compound. We also note that vacancies in a site diluted Kitaev model are predicted to increase the local susceptibility [53, 54, 58]. In the parent compound the field-dependent magnetization at 2 K shows an upward curvature approaching the suppression of the zigzag phase near 7.5 T [14, 22]. For $x > 0.09$, the field-dependent magnetization curves in Fig. 1(b) develop opposite concavity from the clean limit. Interestingly, this coincides with the region of increase in the low temperature susceptibility mentioned above.

The downward trend in $T_{N1}$and T_{N2} with x is also reflected in specific heat measurements (Fig. 1c). The lattice contribution in all cases can be described by $C_p \propto T^2$, an approximation of the 2D Debye law characteristic of the parent compound [13] and other van der Waals bonded materials [70]. The 2D character of the materials is thus not strongly affected by Ir substitution. Weak low temperature features with a magnetic origin (evidenced by magnetic field dependence) are observed at larger x of 0.2 and 0.3 [see SI, Fig. S11], however the absence of a λ - like anomaly indicates no long-range ordering transition above 2 K.

The magnetic ground state of lightly-substituted crystals with $x \leq 0.06$ was characterized by neutron diffraction using the HB-1A and HB-3A beamlines at HFIR, ORNL. Similar to the parent compound with stacking faults, Ir substituted crystals show transitions at T_{N1} with (trigonal notation) $\mathbf{Q}_1 = (1/2\ 0\ 1)$ and T_{N2} with $\mathbf{Q}_2 = (1/2\ 0\ 3/2)$ [13, 36], corresponding, respectively to ABC and ABAB magnetic layer stacking. For $x = 0.035$ (Fig. 2a,b) the relative peak intensities $I(\mathbf{Q}_1)/I(\mathbf{Q}_2) \simeq 6$ at 1.5 K show that the majority of the sample adopts the ABC-type phase. The observed T_{N1} of $\simeq 5.5$ K is consistent with χ and C_p for similarly doped samples. Measurements using the four-circle diffractometer at HB-3A were refined to yield an ordered moment of 0.32(2) μ_B/Ru in the ABC zigzag phase, corresponding to two-thirds of the ordered moment at $x = 0$ [23]. An extensive survey of reciprocal space did not reveal additional peaks associated with alternative magnetically ordered states in the H-K-Γ phase diagram [24].

Increasing the Ir content to $x = 0.06$ (Fig. 2c,d) strongly affects T_N as well as the relative intensities at the two magnetic wavevectors. The (1/2 0 1) peak is absent at 4 K (Fig. 2c) and acquires significant intensity only below 1.6 K. The relative amount of the ABC phase is greatly reduced, leading to $I(\mathbf{Q}_1)/I(\mathbf{Q}_2) \simeq 0.7$ at 0.3 K. No additional peaks characteristic of other candidate magnetic structures were observed in the (H 0 L) scatter-

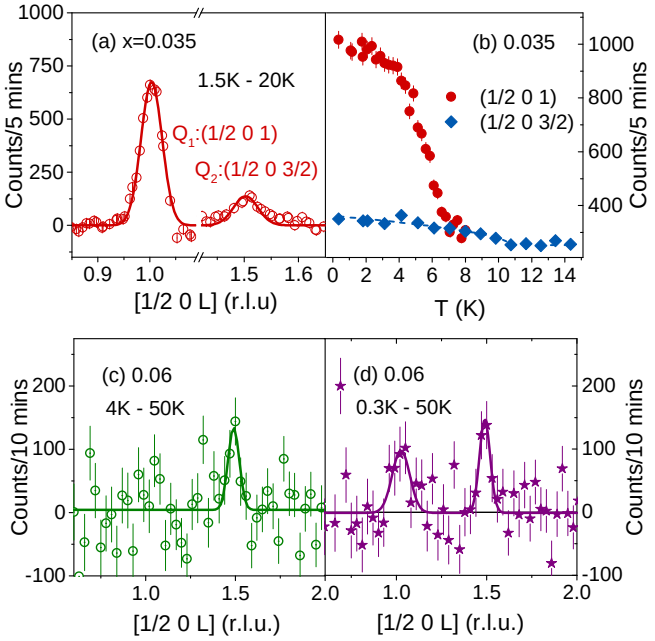

FIG. 2. (a) Scan at 1.5 K collected at HB-1A along [1/2 0 L] through characteristic magnetic reflections $\mathbf{Q}_1$ =(1/2 0 1) and $\mathbf{Q}_2$ =(1/2 0 3/2) for a 50 mg single crystal with $x = 0.035$. 20 K ($T > T_N$) data are subtracted as a background. (b) Temperature scans of the scattering intensity at $\mathbf{Q}_1$ and $\mathbf{Q}_2$. Scans along [1/2 0 L] at (c) 4 K and (d) 0.3 K in a 20 mg single crystal with $x = 0.06$. 50 K data are subtracted as a background.

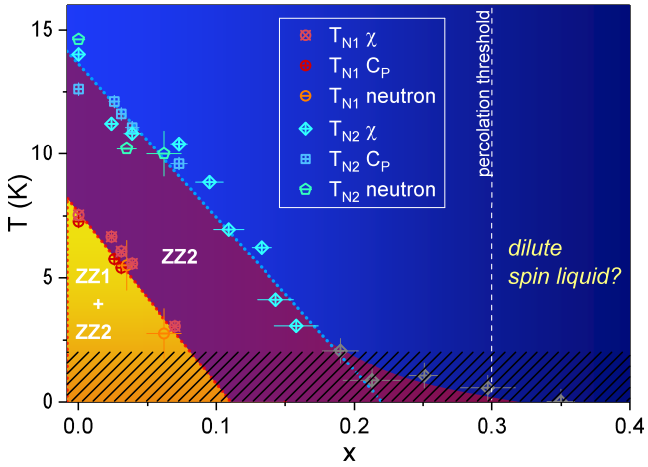

FIG. 3. Phase diagram of $Ru_{1-x}Ir_xCl_3$. Transition temperatures T_{N1} (red symbols) and T_{N2} (blue symbols) determined from magnetic susceptibility, heat capacity, and neutron diffraction mark the boundaries of the ABC-stacked (ZZ1) and ABAB-stacked (ZZ2) zigzag phases in multiphase single crystals. Linear fitting to $T_N(x)$ (dotted lines) gives a critical dilution level for $T_{N1} \to 0$ of $x \sim 0.11$. The cusp at T_{N2} is driven below the experimental base temperature of 2 K (indicated by hashmarks) by $x \simeq 0.2$; at larger x T_{N2} is estimated by extrapolation to $d\chi/dT = 0$ (grey symbols).

ing plane. There is thus no evidence for the emergence of a new magnetically ordered phase as the ABC-type zigzag order is suppressed in the dilute system.

A phase diagram of the $Ru_{1-x}Ir_xCl_3$ system is summarized in Fig. 3. Linear fits to the normalized critical temperatures give initial suppression rates [71] $-d[T_{Ni}/T_{Ni}(0)]/dx = 8.1(7)$ for T_{N1} and 4.4(3) for T_{N2}. The more sensitive response to magnetic site dilution in the ABC phase may be related to a higher degree of frustration in magnetic interactions for 3-layer magnetic stacking than for 2-layer stacking, as evidenced by the different T_N values for the two phases in the parent compound. Extrapolating linearly from small x, the suppression of T_{N1} and T_{N2} to $T = 0$ occurs at $x \simeq 0.11$ and $x \simeq 0.22$, respectively. Above $x \simeq 0.2$, T_{N2} falls below the base temperature of 2 K for susceptibility measurements. However, extrapolation of $d\chi/dT$ to zero indicates that T_{N2} may not vanish until the percolation threshold is crossed (grey symbols, Fig. 3).

The nature of the magnetic ground state in $Ru_{1-x}Ir_xCl_3$ can be further revealed via examination of the excitation spectrum using inelastic neutron scattering (INS). The existing Ir-substituted single crystals are too small for INS experiments and have coexisting magnetic ground states. On the other hand, powders exhibit only the ABAB type ordering [13]. The 14 K (T_{N2}-type) transition in polycrystalline $RuCl_3$ becomes suppressed by $x \simeq 0.3$, similar to the trend in T_{N2} for the single crystals (SI, Fig. S3). The SEQUOIA time-of-flight spectrometer at the Spallation Neutron Source (SNS) was used to measure the response of powders with $x = 0$, 0.05, and 0.35 (Fig. 4). The INS spectrum of $RuCl_3$ ($x = 0$) shows two magnetic features [13] (Fig. 4a). The lower feature M1 arises from zigzag ordered state spin waves and vanishes above T_{N2}. In contrast, the temperature-dependence and energy width of the upper feature M2 $\simeq$6 meV are incompatible with spin-wave theory, but resemble the calculated spectrum for fractionalized excitations of the pure Kitaev QSL model [13, 36, 40].

Ir substitution affects M1 most strongly as seen in Fig. 4(a-c). The energy dependence of the scattering intensity normalized by sample mass and integrated over the Q range [0.5,1] $Å^{-1}$ is shown at $T = 5$ K (Fig. 4d) and $T = 15$ K (Fig. 4e). At 5 K the modes M1 and M2 are clearly visible for $x = 0$, and M1 is gapped. For $x = 0.05$, with $T_{N2} \simeq 10$ K, both modes are also observed, although M1 is broadened and renormalized downwards, and no M1 gap is visible as significantly more scattering is observed at low frequencies. In contrast, the $x = 0.35$ sample, which is magnetically disordered, shows only one broad feature peaked near M2. At 15 K, above T_{N2} for both $x = 0$ and $x = 0.05$, the M1 peak disappears as expected since it arises from spin waves associated with zigzag order. On the other hand, for all three concentrations the M2 feature remains robust, with very little temperature dependence.

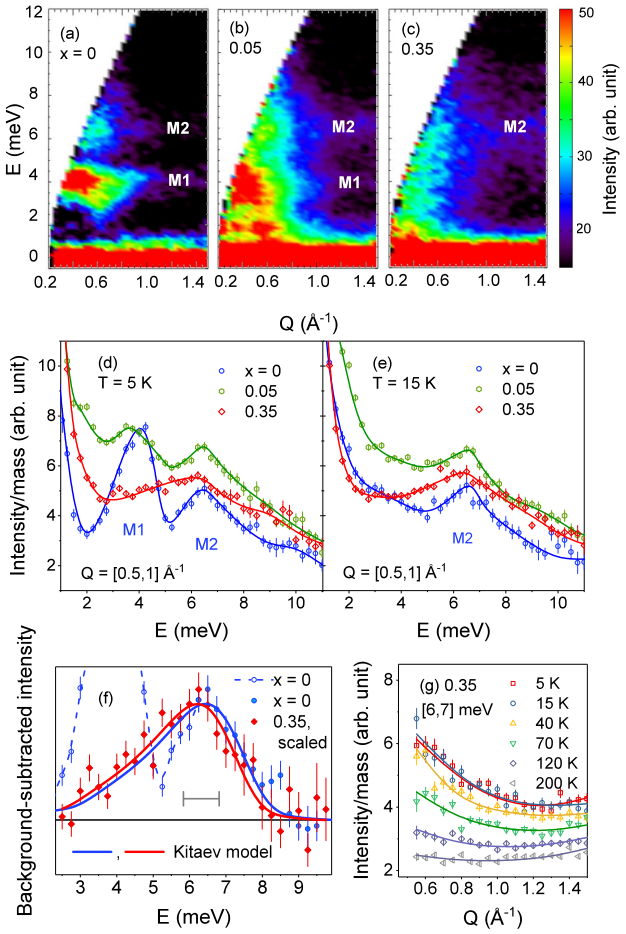

FIG. 4. Powder inelastic scattering of $Ru_{1-x}Ir_xCl_3$ measured at SEQUOIA with Ei = 25 meV. The background from Al sample cans is subtracted from all data, and a correction for the increasing absorption cross section with Ir content is applied to allow direct comparison of intensities. (a)-(c) 2D spectra at 5 K (x values indicated). Constant-Q cuts integrated over Q = [0.5,1]Å^{-1} are shown at (d) 5 K and (e) 15 K. Solid lines are a guide to the eye. The data in (d,e) are normalized by sample mass; see Supplementary Section V for a discussion of the data normalized per Ru ion. (f) Constant-Q cuts at 5 K for $x = 0$ and $x = 0.35$ after subtraction of a linear background. The $x = 0.35$ data have been scaled by a factor of 1.6 to match the height of the $x = 0$ data. Solid blue and red lines represent the calculated scattering of the upper mode of the Kitaev model convoluted with experimental resolution (grey bar) for $x = 0$ and $x = 0.35$, respectively. At low energies the scattering in the magnetically ordered parent compound departs from the model (open symbols, dashed line). (g) Constant-energy cuts at the M2 peak position of [6,7] meV for $x = 0.35$ normalized by $n(\omega) + 1$ to account for the temperature dependence of phonon contamination at low Q. Solid lines are a guide to the eye.

Figure 4(f) shows the constant-Q cuts for $x = 0$ and $x = 0.35$ at 5 K after the subtraction of a linear background. The width of the M2 scattering feature is very broad compared with instrumental resolution. It was shown previously that the scattering on the high-energy side of the M2 mode for $x = 0$ [13] bears a strong resemblance to that calculated for the isotropic antiferromagnetic Kitaev model at Q = 0 [40] (blue line, Fig. 4f). The red line in Fig. 4(f) is a fit of the $x = 0.35$ data to this model over the full energy range of the M2 feature, showing very good agreement with a value of the Kitaev energy scale $K = 5.3(2)$ meV.

The Q dependence of the scattering in the vicinity of the M2 mode in the $x = 0.35$ system is illustrated in Fig. 4(g), with the data normalized by $(1 - e^{-E/k_BT})^{-1}$. The signal exhibits little change up to moderate temperatures, consistent with expectations for a QSL with the energy scale set by K [72]. However, for higher temperatures the scattering shows a stronger temperature dependence than the pure material [13, 36], suggesting that the excitations in the dilute system are more fragile.

The energy, temperature, and wave-vector dependence of the spectrum at $x = 0.35$ are all consistent with expectations for fractionalized excitations, suggesting that the $T = 0$ ground state is effectively a QSL. In the pure Kitaev model spin-spin correlations do not extend beyond nearest neighbors, and thus are relatively insensitive to non-magnetic dilution. Therefore it is reasonable that these correlations and their associated excitations exist beyond the percolation threshold for long-range order. Excitations in Kitaev systems with mobile holes have been predicted to form bound states [59, 60], which one might expect to manifest as sharp peaks in the magnetic response function. No such peaks are observed in the present experiment, however this is not surprising as the nonmagnetic Ir^{3+} impurities here are completely static and do not introduce any change in charge neutrality to the system.

In summary, incorporating Ir^{3+} into $Ru_{1-x}Ir_xCl_3$ decreases the Néel temperatures of the ordered magnetic phases, while leaving intact the broad upper excitation mode associated with fractionalized excitations in the $x = 0.05$ and $x = 0.35$ compositions investigated by INS. Above the percolation threshold where long-range order is absent, the fractionalized excitations dominate the spectrum and the low-temperature region may effectively be a dilute QSL. The robust nature of such QSL physics in $RuCl_3$ with respect to chemical substitution strongly motivates further investigation of dopants, in particular those that would introduce mobile charge carriers, an avenue which is predicted to bring about exotic superconductivity [43–49].

Acknowledgments

P.L.K and D.M. were supported by the Gordon and Betty Moore Foundations EPiQS Initiative Grant GBMF4416. J.-Q.Y. and C.A.B. acknowledge support from the U.S. DOE, Office of Science, Basic Energy Sciences, Materials Sciences and Engineering Division. The work at ORNL HFIR and SNS was sponsored by the Scientific User Facilities Division, Office of Basic Energy Sciences, U.S. DOE. We thank I. McKenzie for support at TRIUMF, B. Chakoumakos and F. Ye for assistance with XRD, and B. Sales, M. McGuire, and A. May for

helpful discussions.

[1] L. Balents, Nature **464**, 199 (2010).
[2] L. Savary and L. Balents, Rep. Prog. Phys. **80**, 016502 (2017).
[3] C. Nayak, S. H. Simon, A. Stern, M. Freedman, and S. Das Sarma, Rev. Mod. Phys. **80**, 1083 (2008).
[4] A. Y. Kitaev, Annals of Physics **303**, 2 (2003).
[5] A. Kitaev, Annals of Physics **321**, 2 (2006).
[6] G. Jackeli and G. Khaliullin, Phys. Rev. Lett. **102**, 017205 (2009).
[7] Y. Singh and P. Gegenwart, Phys. Rev. B **82**, 064412 (2010).
[8] Y. Singh, S. Manni, J. Reuther, T. Berlijn, R. Thomale, W. Ku, S. Trebst, and P. Gegenwart, Phys. Rev. Lett. **108**, 127203 (2012).
[9] S. Hwan Chun, J.-W. Kim, J. Kim, H. Zheng, C. C. Stoumpos, C. D. Malliakas, J. F. Mitchell, K. Mehlawat, Y. Singh, Y. Choi, T. Gog, A. Al-Zein, M. M. Sala, M. Krisch, J. Chaloupka, G. Jackeli, G. Khaliullin, and B. J. Kim, Nat Phys **11**, 462 (2015).
[10] J. Chaloupka and G. Khaliullin, Phys. Rev. B **94**, 064435 (2016).
[11] K. W. Plumb, J. P. Clancy, L. J. Sandilands, V. V. Shankar, Y. F. Hu, K. S. Burch, H.-Y. Kee, and Y.-J. Kim, Phys. Rev. B **90**, 041112 (2014).
[12] H.-S. Kim, V. S. V., A. Catuneanu, and H.-Y. Kee, Phys. Rev. B **91**, 241110 (2015).
[13] A. Banerjee, C. A. Bridges, J.-Q. Yan, A. A. Aczel, L. Li, M. B. Stone, G. E. Granroth, M. D. Lumsden, Y. Yiu, J. Knolle, S. Bhattacharjee, D. L. Kovrizhin, R. Moessner, D. A. Tennant, D. G. Mandrus, and S. E. Nagler, Nature Materials **15**, 733 (2016).
[14] Y. Kubota, H. Tanaka, T. Ono, Y. Narumi, and K. Kindo, Phys. Rev. B **91**, 094422 (2015).
[15] M. Majumder, M. Schmidt, H. Rosner, A. A. Tsirlin, H. Yasuoka, and M. Baenitz, Phys. Rev. B **91**, 180401 (2015).
[16] J. A, Sears, Y. Zhao, Z. Xu, J. W. Lynn, and Y.-J. Kim, Phys. Rev. B **95**, 180411(R) (2017).
[17] X. Liu, T. Berlijn, W.-G. Yin, W. Ku, A. Tsvelik, Y.-J. Kim, H. Gretarsson, Y. Singh, P. Gegenwart, and J. P. Hill, Phys. Rev. B **83**, 220403 (2011).
[18] F. Ye, S. Chi, H. Cao, B. C. Chakoumakos, J. A. Fernandez-Baca, R. Custelcean, T. F. Qi, O. B. Korneta, and G. Cao, Phys. Rev. B **85**, 180403 (2012).
[19] S. K. Choi, R. Coldea, A. N. Kolmogorov, T. Lancaster, I. I. Mazin, S. J. Blundell, P. G. Radaelli, Y. Singh, P. Gegenwart, K. R. Choi, S.-W. Cheong, P. J. Baker, C. Stock, and J. Taylor, Phys. Rev. Lett. **108**, 127204 (2012).
[20] S. C. Williams, R. D. Johnson, F. Freund, S. Choi, A. Jesche, I. Kimchi, S. Manni, A. Bombardi, P. Manuel, P. Gegenwart, and R. Coldea, Phys. Rev. B **93**, 195158 (2016).
[21] J. A. Sears, M. Songvilay, K. W. Plumb, J. P. Clancy, Y. Qiu, Y. Zhao, D. Parshall, and Y.-J. Kim, Phys. Rev. B **91**, 144420 (2015).
[22] R. D. Johnson, S. C. Williams, A. A. Haghighirad, J. Singleton, V. Zapf, P. Manuel, I. I. Mazin, Y. Li, H. O. Jeschke, R. Valenti, and R. Coldea, Phys. Rev. B **92**, 235119 (2015).
[23] H. B. Cao, A. Banerjee, J.-Q. Yan, C. A. Bridges, M. D. Lumsden, D. G. Mandrus, D. A. Tennant, B. C. Chakoumakos, and S. E. Nagler, Phys. Rev. B **93**, 134423 (2016).
[24] J. G. Rau, E. K.-H. Lee, and H.-Y. Kee, Phys. Rev. Lett. **112**, 077204 (2014).
[25] J. Reuther, R. Thomale, and S. Rachel, Phys. Rev. B **90**, 100405 (2014).
[26] J. Chaloupka, G. Jackeli, and G. Khaliullin, Phys. Rev. Lett. **110**, 097204 (2013).
[27] J. Chaloupka and G. Khaliullin, Phys. Rev. B **92**, 024413 (2015).
[28] J. Chaloupka, G. Jackeli, and G. Khaliullin, Phys. Rev. Lett. **105**, 027204 (2010).
[29] Y. Sizyuk, C. Price, P. Wolfle, and N. B. Perkins, Phys. Rev. B **90**, 155126 (2014).
[30] Y. Sizyuk, P. Wolfle, and N. B. Perkins, Phys. Rev. B **94**, 085109 (2016).
[31] R. Yadav, N. A. Bogdanov, V. M. Katukuri, S. Nishimoto, J. v. d. Brink, and L. Hozoi, Sci. Rep. **6**, 37925 (2016).
[32] V. M. Katukuri, S. Nishimoto, V. Yushankhai, A. Stoyanova, H. Kandpal, S. Choi, R. Coldea, I Rousochatzakis, L. Hozoi, and J. v. d. Brink, New J. Phys. **16**, 013056 (2014).
[33] K. Foyevtsova, H. O. Jeschke, I. I. Mazin, D. I. Khomskii, and R. Valenti, Phys. Rev. B **88**, 035107 (2013).
[34] S. M. Winter, Y. Li, H. O. Jeschke, and R. Valenti, Phys. Rev. B **93**, 214431 (2016).
[35] K. Shinjo, S. Sota, and T. Tohyama, Phys. Rev. B **91**, 054401 (2015).
[36] A. Banerjee, J.-Q. Yan, J. Knolle, C. A. Bridges, M. B. Stone, M. D. Lumsden, D. G. Mandrus, D. A. Tennant, R. Moessner, and S. E. Nagler, Science **365**, 1055 (2017).
[37] L. J. Sandilands, Y. Tian, K. W. Plumb, Y.-J. Kim, and K. S. Burch, Phys. Rev. Lett. **114**, 147201 (2015).
[38] J. Nasu, J. Knolle, D. L. Kovrizhin, Y. Motome, and R. Moessner, Nat Phys **12**, 912 (2016).
[39] S. Nath Gupta, P. V. Sriluckshmy, K. Mehlawat, A. Balodhi, D. K. Mishra, S. R. Hassan, T. V. Ramakrishnan, D. V. S. Muthu, Y. Singh, and A. K. Sood, Europhys. Lett. **114**, 47004 (2016).
[40] J. Knolle, D. Kovrizhin, J. Chalker, and R. Moessner, Phys. Rev. Lett. **112**, 207203 (2014).
[41] J. Knolle, G.-W. Chern, D. Kovrizhin, R. Moessner, and N. Perkins, Phys. Rev. Lett. **113**, 187201 (2014).
[42] B. Perreault, J. Knolle, N. B. Perkins, and F. J. Burnell, Phys. Rev. B **94**, 104427 (2016).
[43] T. Hyart, A. R. Wright, G. Khaliullin, and B. Rosenow, Phys. Rev. B **85**, 140510(R) (2012).
[44] Y.-Z. You, I. Kimchi, and A. Vishwanath, Phys. Rev. B **86**, 085145 (2012).
[45] J.-W. Mei, Phys. Rev. Lett. **108**, 227207 (2012).
[46] S. Okamoto, Phys. Rev. Lett. **110**, 066403 (2013).
[47] S. Okamoto, Phys. Rev. B **87**, 064508 (2013).
[48] F. Trousselet, P. Horsch, A. M. Ole, and W.-L. You, Phys. Rev. B **90**, 024404 (2014).
[49] L. Kimme, T. Hyart, and B. Rosenow, Phys. Rev. B **91**, 220501(R) (2015).
[50] F. Zschocke and M. Vojta, Phys. Rev. B **92**, 014403 (2015).
[51] J. Brennan and J. Vala, J. Phys. Chem. A **120**, 3326 (2016).
[52] K. Dhochak, R. Shankar, and V. Tripathi, Phys. Rev. Lett. **105**, 117201 (2010).

[53] A. J. Willans, J. T. Chalker, and R. Moessner, Phys. Rev. Lett. **104**, 237203 (2010).
[54] A. J. Willans, J. T. Chalker, and R. Moessner, Phys. Rev. B **84**, 115146 (2011).
[55] S. G., V. Sreenath, A. Lakshminarayan, and R. Narayanan, Phys. Rev. B **85**, 054204 (2012).
[56] E. C. Andrade and M. Vojta, Phys. Rev. B **90**, 205112 (2014).
[57] G. J. Sreejith, S. Bhattacharjee, and R. Moessner, Phys. Rev. B **93**, 064433 (2016).
[58] F. Trousselet, G. Khaliullin, and P. Horsch, Phys. Rev. B **84**, 054409 (2011).
[59] G. B. Halasz, J. T. Chalker, and R. Moessner, Phys. Rev. B **90**, 035145 (2014).
[60] G. Halasz and J. T. Chalker, Phys. Rev. B **94**, 235105 (2016).
[61] K. Mehlawat, G. Sharma, and Y. Singh, Phys. Rev. B **92**, 134412 (2015).
[62] S. Manni, Y. Tokiwa, and P. Gegenwart, Phys. Rev. B **89**, 241102(R) (2014).
[63] G. Cao, T. F. Qi, L. Li, J. Terzic, V. S. Cao, S. J. Yuan, M. Tovar, G. Murthy, and R. K. Kaul, Phys. Rev. B **88**, 220414(R) (2013).
[64] S. Manni, S. Choi, I. I. Mazin, R. Coldea, M. Altmeyer, H. O. Jeschke, R. Valenti, and P. Gegenwart, Phys. Rev. B **89**, 245113 (2014).
[65] K. Rolfs, S. Toth, E. Pomjakushina, D. Sheptyakov, J. Taylor, and K. Conder, Phys. Rev. B **91**, 180406(R) (2015).
[66] K. Brodersen, F. Moers, and H. Schnering, Naturwissenschaften **52**, 205 (1965).
[67] X. Feng, Y. Deng, and H. Blote, Phys. Rev. E **78**, 031136 (2008).
[68] P. D. d. Rotier, and A. Yaouanc, J. Phys. Condens. Matter **9**, 9113 (1997).
[69] F. Lang, P. J. Baker, A. A. Highighirad, Y. Li, D. Prabhakaran, R Valenti, and S. J. Blundell, Phys. Rev. B **94**, 020407 (2016).
[70] J. Krumhansl and H. Brooks, J. Chem. Phys. **21**, 1663 (1953).
[71] S.-W. Cheong, A. S. Cooper, L. W. Rupp, B. Batlogg, J. D. Thompson, and Z. Fisk, Phys. Rev. B **44**, 9739 (1991).
[72] J. Nasu, M. Udagawa, and Y. Motome, Phys. Rev. B **92**, 115122 (2015)
.